PHOTONIC CRYSTAL FIBER MODE CHARACTERIZATION WITH MULTIPOLE METHOD

Dana Georgeta POPESCU[1], Paul STERIAN[2]

Photonic crystal fibers (PCFs) have shown great capacity in overcoming the limits of conventional fibers and obtaining remarkable results the regular fiber cannot achieve, such as high nonlinear effects, controlled dispersion, low bending losses, low losses and high power transmittance. In this paper we considered a PCF having N inclusions and a hole-diameter of $d/a = 0.3$. *For different values of the wavelength varying between 1 μm to 2 μm and for different pitch size we studied the fundamental mode of a PCF having the refractive index of the cylinders* $n_c = 1$ *(air) and a silica background with the multipole method. This method takes into account both the real and imaginary parts of the mode propagation constant, providing information about losses using Bloch transform. It allows a clear distinction between cladding and defect modes and it is highly stable when varying the fiber parameters and wavelength.*

Keywords: photonic crystal fiber, multipole method, field distribution, Bloch transform.

1. Introduction

The first photonic crystal fiber (PCF) was realized after the prediction of Birks *et al.* [1] in 1995. They highlight the guidance of the light through PBG (photonic bang gap) effects in a hollow core along the length of a fiber with air holes, which lead to the first PCF [2] that had remarkable properties such as unprecedented dispersion [3], endlessly single mode guidance [4] and nonlinear properties. These interesting features have led to multiple novel applications. PCFs are attracting tremendous attention in recent years because of their important properties and unique propagation characteristics that cannot be realized with conventional optical fibers, incorporating a larger refractive index contrast and requiring a complete electromagnetic treatment rather than a weak guidance approximation [5-8]. PCF became a major topic of research because they have allowed technological breakthrough, permitting the discovery of new physical phenomena and unveiling new aspects of wave guidance. Endlessly single mode fibers or hollow core guidance made possible the development of novel application in sensing, metrology, nonlinear optics, and particle guidance or dispersion management [9-12]. In cross-section, a photonic crystal fiber appears as a periodic structure of dielectric materials, commonly a solid silica material

[1], PhD Student, University POLITEHNICA of Bucharest, Romania, e-mail: dana.popescu@infim.ro
[2] Prof., Faculty of Applied Sciences, University POLITEHNICA of Bucharest, Romania, Romania

pierced by air holes grouped in a triangular lattice that extends parallel to the fiber axes. The creation of a defect leads to an enhanced propagation of the light through this periodic lattice. One type of MOF has a central air hole and confines light in it by PBG effects making possible the propagation of the light in air. However the location of the modes which propagates in this kind of fiber represents a numerically difficult task. Another type of MOF is the one with silica core, which allows the propagation of the light by means of modified total internal reflection. To guide the design process precise numerical simulations are essentials for reduction of the costs and the effort needed for the fabrication of photonic crystal fibers. In this paper we determine the fundamental mode for a PCF structure that is studied by numerical simulation based on multipole method [13-14].

2. Method

Lately, remarkable progress has been made in the design and manufacture of MOFs in an area of new applications as dispersion compensation and light guiding in air. The finding and analyzing of PCF modes properties was possible due to sophisticated numerical method called multipole method.

Multipole method is part of the important class of computational and theoretical techniques used for photonic crystal (PhC) structures study, a numerical formulation that developed the mode finding of holey fibers, being useful as a mode solver. It concerns the both real and imaginary parts of the mode propagation constant, providing information about losses and it is used for full vector modal calculation of photonic band gap fibers, achieving rapid convergence and high accuracy with modest computing resources. A freely software is available [15] that implements this method for circular inclusions and can be extended for the noncircular ones. In practice it deals with two types of PCF: solid core PCF and air core PCF, surrounded by air holes, permitting the modeling of a large number of inclusions, calculation time being reduced for a structure with discrete rotational symmetry by capitalization of symmetry properties of the modes.

To represent the electromagnetic field, the multipole method uses two different kind of field expansion: the first one, the local expansion, which is valid just outside each inclusion, is related to the field components that are scattered away by the inclusions, being incident on them. The second one is valid along the different parts of the structure.

The electromagnetic field must satisfy boundary conditions at the margins of each inclusion which are given by the Maxwell's equation. So we can find a relation between the coefficients of expansions defined on the opposite side of the boundary and another one by applying the Rayleigh identity, obtaining a homogeneous system of algebraic equations in one of the coefficients only that

can be expressed in a matrix form which depends on the propagation constant of the mode that is propagation in PCF. Therefore we can reduce the problem of finding modes that propagates in the photonic structure in a solution discovery corresponding to finding the propagation constant.

Considering the balance of incoming and outgoing fields we can solve the problem of scattering consisting of multipole inclusions [7, 13-14]. If we consider a single inclusion in the matrix that can be seen in Fig. 1, the field being $U(r,\theta+2\pi)=U(r,\theta)$ periodic along the angular coordinate, we can expand $U(r,\theta)$ in a Fourier series fixing r:

$$U(r,\theta)=\sum_{n\in Z} f_n(r)e^{in\theta} \tag{1}$$

In relation (1), the Fourier coefficients $f_n(r)$ are regular functions of r.
For the Helmholtz equation,

$$\left(\Delta+k_1^2\right)U=0 \tag{2}$$

where $k_1^2=k^2n_1^2-\beta^2$, k is the free space wave number, β is the propagation constant, n_1 is the real refractive index, by Fourier expansion we obtain:

$$\sum_{n\in Z}\left(\frac{\partial^2 f_n(r)}{\partial r^2}+\frac{1}{r}\frac{\partial f_n(r)}{\partial r}+\left(k_1^2-\frac{n^2}{r^2}\right)f_n(r)\right)e^{in\theta}=0 \tag{3}$$

Because $U(r,\theta)$ is a continuous function, one obtains

$$\frac{\partial^2 f_n(v)}{\partial v^2}+\frac{1}{v}\frac{\partial f_n(v)}{\partial v}+\left(1-\frac{n^2}{v^2}\right)f_n(v)=0 \tag{4}$$

standing for all n where $v=k_1r$. This equation is the Bessel differential equation of order n.

The functions

$$f_n(v)=C_nJ_n(v)+D_nH_n(v) \tag{5}$$

are linear combination of Bessel functions of the first and second kind of order n ($J_n(v),Y_n(v)$) or of Bessel and Hankel functions of the first kind of order n ($H_n(v)=J_n(v)+iY_n(v)$).

The expression

$$U(r,\theta)=\sum_{n\in Z}\left(C_nJ_n(k_1r)+D_nH_n(k_1r)\right)e^{in\theta} \tag{6}$$

is called a Fourier Bessel series.

The Fourier Bessel series can be split in two parts: the Bessel functions of the first kind (regular everywhere) and the Hankel functions (they have a singularity at 0). When we consider no inclusions, the whole space is homogeneous. A source placed beyond the outer ring (S_0) radiates a field which is

regular in the region delimited by the inner circle and its field expansion can only contain Bessel functions. In this manner $U(r,\theta)$ becomes:

$$U(r,\theta) = R(r,\theta) + O(r,\theta) \tag{7}$$

with

$$R(r,\theta) = \sum_{n\in Z} C_n J_n(k_1 r) e^{in\theta} \tag{8}$$

the regular part of U and

$$O(r,\theta) = \sum_{n\in Z} D_n H_n(k_1 r) e^{in\theta} \tag{9}$$

its singular counterpart.

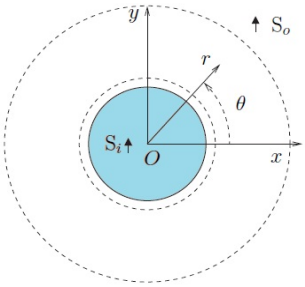

Fig. 1. Single inclusion in the matrix where $S_{i,o}$ are sources.

For an inclusion, the field reaching it will be scattered. S_o, R and O are linked by a linear scattering operator S, where $O=SR$. S is represented by a matrix which links the Fourier Bessel coefficients C_n with R and D_n with O. For two inclusions the incoming field for inclusion 1 results from the superposition of the field radiated from S_o and the scattered field from inclusion 2 and similarly for the incoming field for inclusion 2.

3. Results and discussion

We are interested in PCFs having the inclusions in the nodes of a periodic lattice, their properties being closely related to the cladding's band structure. We used a discrete Fourier transformation on specific points along the structure to isolate the Bloch components for a mode.

We considered a PCF having N inclusions centered around position vectors c_j ($l \in [1...N]$). Supposing that the positions are defined by a finite subset of a periodic lattice, we can generate a Bloch transform of a given PCF mode by choosing a number of $B_m(c_j)$ quantities which can characterize the complex field amplitudes for each N inclusion. In multipole formulation this quantities are

considered to be the multipole's amplitudes occurring in the E_z and H_z expansion. We define the Bloch transform for B_m quantities:

$$B_m(k) = \sum_{j=1}^{N} e^{-ikc_j} B_m(c_j) \quad (10).$$

Bloch transform term is usually used in Bloch-Floquet theory. If a mode consist from a superposition of N_B Bloch waves having k_{B}^n Bloch vectors and the field distribution satisfy $V(r) = \sum_{n=1}^{N_{\mathbf{B}}} e^{ik_B^n r} v_{k_B^n}(r)$, where $v_{k_B^n}(r)$ function has the lattice periodicity, the $B_m(c_j)$ quantities satisfy $B_m(c_j) = \sum_{n=1}^{N_B} e^{ik_B^n c_j} \hat{B}_m^n$, where $\hat{B}_m^n$ is the complex amplitude of Bloch wave associated k_{B}^n Bloch vector in $B_m(c_j)$ decomposition.

For a given mode the important information obtained from Bloch transform can be visualized plotting $|B_m(k)|$ vs. *k*. We can find the total Bloch transform summing over transformations of all representative quantities:

$$B^T(k) = \sum_m \frac{1}{\sup_{k' \in \Re^2} |B_m(k')|} |B_m(k)| \quad (11)$$

All Bloch transform and field distribution figures are depict in a normalized, linear color scale, as in Fig. 2. The darkest color represents the smallest value of the distribution within the drawn frame and the brightest one represents the maximum value.

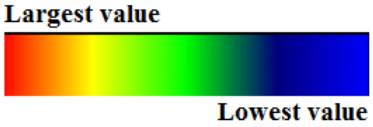

Fig. 2. Color scale used for Bloch transform plots and field distribution.

The total Bloch transform was computed with the E_z Bessel Fourier coefficients, but the transform has the same graphical accuracy when calculated with H_z coefficients. The symmetry properties of the mode induce the symmetry properties of the Bloch transform.

In *Tables 1* to *4*, using the Bloch transform we identified modes of PCFs with different but comparable structures. These lines of contour plots relate to the fundamental mode of a PCF with N_r=*4* holes of air inclusions in silica, with the same relative hole size *d/a=0.3*, but with different values of the wavelength from *1 μm* to *2 μm* and with different pitch.

Comparing the figures from *Tables 1* to *3* with the ones in *Table 4* we observe that the Bloch transform remains similar for the two values of the pitch (*0.254 μm* and *2.3 μm*) even if the field patterns differ considerably, being only one peak centered on *k=0*. For the wider mode the width of the peak changes, being much narrower than for the well confined mode. Nevertheless, the shape of the Bloch transform remains mainly unchanged, supporting the robustness of the mode analysis based on the Bloch transform.

Since the challenge in numerical calculations of physical properties of PCF is to minimize the otherwise time consuming computational costs *i.e* memory load, CPU processing time resulting in efficient manipulation of information acquired in simulations, the Bloch transform approach offers such a solution.

Based on the theorem which states the equivalence of the analysis performed in real space of the field pattern and the reciprocal space analysis of the Bloch transform characteristics, a tremendous reduction in time and computational costs comes together with a high accuracy of the mode analysis in PCF. Its analysis allows in this manner to avoid the more complex and resources consuming attempt of studying the mode propagation based on the direct space methods. The analysis performed in this framework is way less expensive concerning the computational costs, at the end allowing the conversion from Bloch transform to real space shape of the fields, up to a phase factor.

In this context, in *Table 1 - 3* it is well pictured the Heisenberg-type property for Bloch transform correlating it to the finite Fourier transform. The Heisenberg relation links the width of the Bloch transform peaks with the spatial extent of the mode: when the propagating mode is highly collimated, well localized in the real space, the Bloch transform in the reciprocal space is sparse. The most important property of the Bloch transform is the geometric distribution of the peaks, meaning the form of the Bloch transform (the mode characteristic of the PCF), being extremely stable when varying the wavelength and the fiber parameters.

Table 1

Fundamental mode of a photonic crystal fiber with the same pitch $a = 0.254 \mu m$, hole diameter $d / a = 0.3$ and number of rings $N_r = 4$, but with different wavelength. The refractive index of the cylinders is $n_c = 1$ (air) and a silica background

λ(μm)	**1.0**	**1.00005**	**1.1**	**1.2**
n_{Si}	1.45042	1.45042	1.44920	1.44805
$\lvert E_z \rvert$	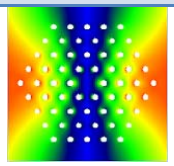	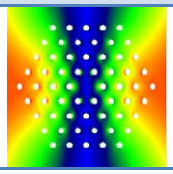	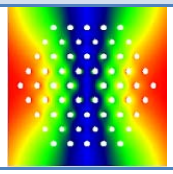	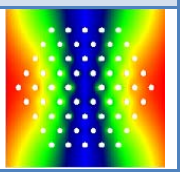

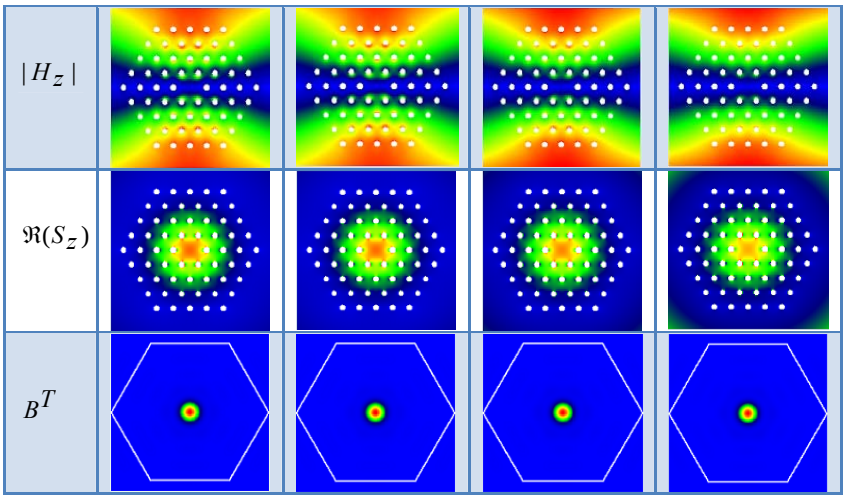

It is known that the field distribution and Bessel-Fourier coefficients of the same mode can vary a lot with the modification of the fiber parameters and because of that it is very difficult to identify the similar modes that have comparable structures. Our simulations revealed that the Bloch transform of a given mode does not change its form even if we modify the fiber parameters and this is the most precise and the most convenient method for defining and differentiating specific modes. This property is very difficult to demonstrate without a clear classification of the modes, but it can be understood due to the decomposition of each mode by the Bloch transform in natural bases of the structure.

Upon a careful analysis of data depicted in *Table 1 - 3* one can easily draw a few conclusions. First of them is that, even small variations of the PBG fiber are reflected in the different propagating patterns of the electric and magnetic fields. This is not surprising since the dependence between the field patterns, dielectric constants and geometric parameters is clearly stated and fixed by the Maxwell equations. A striking fact is that, even when the electric and magnetic field are featured by significant variations, the pattern deduced for the Bloch transform does not change significantly. Based on the Bloch theorem, is easy to understand why it is more convenient to choose in the last representation: it is easier to manipulate it and at the end, the reformulation in the direct space may be realized, allowing for a direct visualization of the field patterns.

Table 2

Fundamental mode of a photonic crystal fiber with the same pitch $a = 0.254\mu m$, hole diameter $d/a = 0.3$ and number of rings $N_r = 4$, but with different wavelength. The refractive index of the cylinders is $n_c = 1$ (air) and a silica background

λ(μm)	**1.3**	**1.4**	**1.5**	**1.6**
n_{Si}	1.44692	1.44560	1.44462	1.44342
$\lvert E_z \rvert$	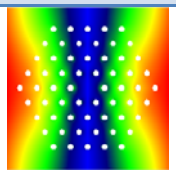	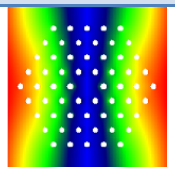	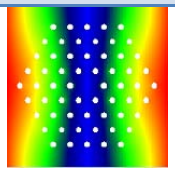	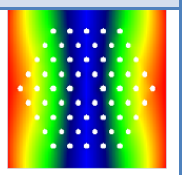
$\lvert H_z \rvert$	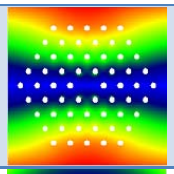	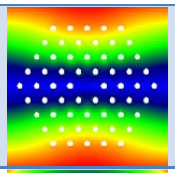	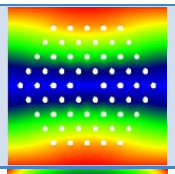	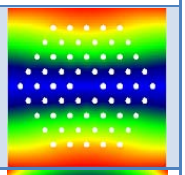
$\Re(S_z)$	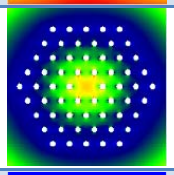	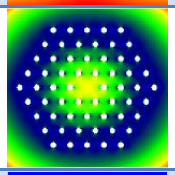	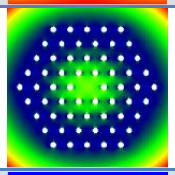	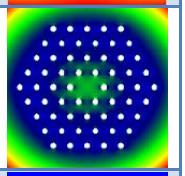
B^T	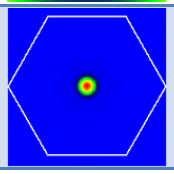	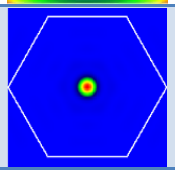	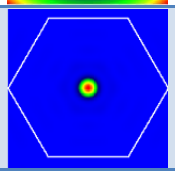	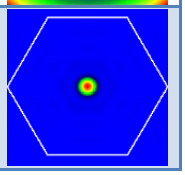

Table 3

Fundamental mode of a photonic crystal fiber with the same pitch $a = 0.254\mu m$, hole diameter $d/a = 0.3$ and number of rings $N_r = 4$, but with different wavelength. The refractive index of the cylinders is $n_c = 1$ (air) and a silica background

λ(μm)	**1.7**	**1.8**	**1.9**	**2.0**
n_{Si}	1.44217	1.44087	1.43951	1.43809
$\lvert E_z \rvert$	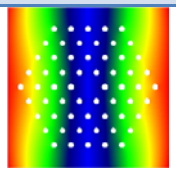	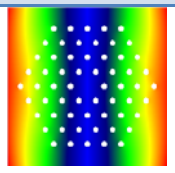	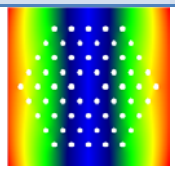	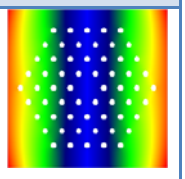

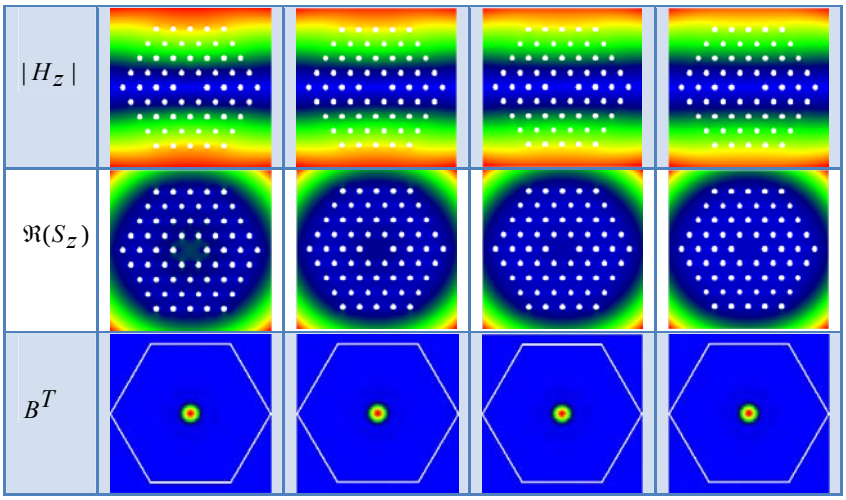

On the other hand, in *Table 4* are depicted the field patterns for a pitch size of $a = 2.3\mu m$. Despite at a brief visual inspection of the Bloch transform we would be tempted to conclude that the differences are only minor compared to the previous cases, the conversion of fields in direct space shows a significant difference. The losses minimized in this latter case, the modes being highly collimated around the center of the PCF.

This result allows on one hand the optimization of dielectric and geometric parameters of PCF in order to minimize the losses and on the other hand proves the efficiency of Bloch transform method in predicting the optical properties of systems with cylindrical symmetry, in particular of photonic band gap fibers.

Table 4

Fundamental mode of a photonic crystal fiber with the same pitch $a = 2.3\mu m$, hole diameter $d/a = 0.3$ and number of rings $N_r = 4$, but with different wavelength. The refractive index of the cylinders is $n_c = 1$ (air) and a silica background

λ(μm	**1.0**	**1.5**	**2.0**
n_{Si}	1.45042	1.44462	1.43809
$\|E_z\|$	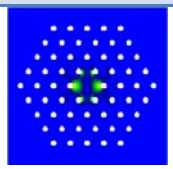	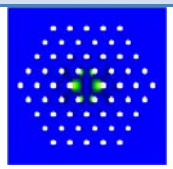	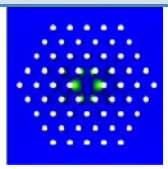

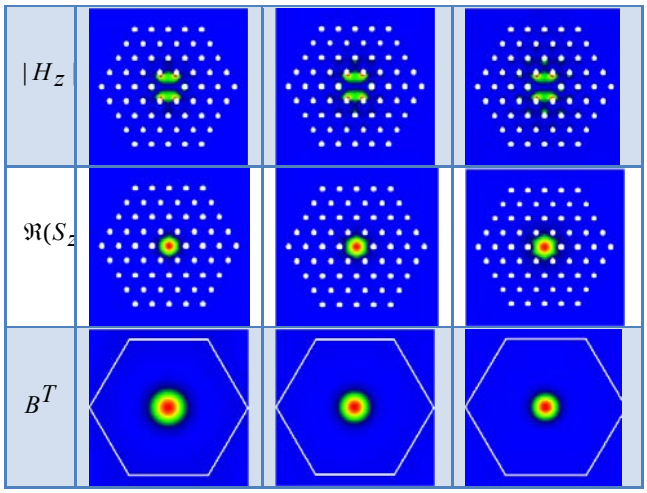

6. Conclusions

In this paper we proved that the Bloch transform method is a very powerful tool for the PCF mode study.

Its analysis in terms of Bloch resonant waves allows a better identification of the modes and allows a clear distinction between cladding and defect modes.

Based on the equivalence between the description of the physical system under study by a direct space approach and a reciprocal space description based on the Bloch transform analysis, we showed that the analysis of the field patterns, symmetry and propagation conditions can be efficiently described, reducing the computational costs significantly. Additionally, the predicted results are highly accurate.

We established under which conditions the losses can be minimized, varying the dielectric and geometric parameters of the PCF.

These results will further furnish the premises for accurate calculations on photonic systems with cylindrical symmetry in order to improve the working parameters of PCF for applications in optical electronics.

Acknowledgements

Project co-financed from FSE through POSDRU 2007-2013, ID76909.

REFERENCES

[1] *T. A. Birks, P. J. Roberts, P. St.J. Russell, D. M. Atkin, and T. J. Shepherd*, "Full 2D photonic band gaps in silica/air structures," Electron. Lett., **Vol. 31**, 1995, pp.1941-1943.

[2] *J.C. Knight, T.A. Birks, P.S.J. Russell, and D.M. Atkin,* "All-silica single-mode optical fiber with photonic crystal cladding," Opt. Lett., **Vol. 21**, 1996, pp.1547-1549.

[3] *D. Mogilevtsev, T. A. Birks, and P. S. J. Russell,* "Dispersion of photonic crystal fibers," Opt. Lett., **Vol. 23**, 1998, pp. 1662-1664.
[4] *T.A. Birks, J.C. Knight, and P.S.J. Russell,* "Endlessly single-mode photonic crystal fiber," Opt. Lett., **Vol. 22**, 1997, pp. 961-963.
[5] *D. Marcuse*, Theory of Dielectric Optical Waveguides, 2nd ed., Chap. 2 Academic, San Diego, Calif., 1991.
[6] *D.G. Popescu, P. Sterian*, "FDTD analysis of photonic crystals with square and hexagonal symmetry," Journal of Advanced Research in Physics, **Vol. 2**, 2011, pp. 1-5.
[7] *D.G. Popescu, P. Sterian,* "Nonlinear Interaction Modeling in Photonic Crystals," Annals of the Academy of Romanian Scientists Series on Science and Technology of Information, **Vol.4** 2011, pp. 105-124.
[8] *D.G. Popescu, P. Sterian,* "FDTD analysis of photonic crystals with square symmetry and defects," INSODE 11-14.05.2012 Conference, Turkey, Procedia Computer Science, in press.
[9] *P. Russell*, "Photonic Crystal Fibers," Science, **Vol. 299**, 2003,pp. 358–362.
[10] *A. Sterian, P. Sterian,* "Mathematical Models of Dissipative Systems in Quantum Engineering**",** Mathematical Problems in Engineering, **vol**. 2012, Article ID 347674, 12 pages, doi:10.1155/2012/347674,(2012).
[11] *A.R. Sterian* "Coherent Radiation Generation and Amplification in Erbium Doped Systems" Advances in Optical Amplifiers, Paul Urquhart (Ed.), ISBN: 978-953-307-186-2, InTech,VIENNA (2011).
[12] *F.S. Iliescu et al.,* "Continuous separation of white blood cell from blood in a microfluidic device", University Politehnica of Bucharest Scientific Bulletin-Series A-Applied Mathematics and Physics, **Vol. 71,** Issue: 4, pp. 21-30**,** 2009.
[13] *T.P. White et al.,* "Multipole method for microstructured optical fibers. I. Formulation," J. Opt. Soc. Am. B, **Vol. 19**, 2002, pp. 2322-2330.
[14] *B.T. Kuhlmey et al.,* "Multipole method for microstructured optical fibers. II. Implementation and results," J. Opt. Soc. Am. B, **Vol. 19**, 2002, pp. 2331-2340
[15] CUDOSMOF: www.cudos.org.au